AN ENDOR INVESTIGATION OF THE V_K CENTER IN $KMgF_3$

By

EUGENE PHILIP LITTLE II

Bachelor of Science

South Dakota State University

Brookings, South Dakota

1974

Submitted to the Faculty of the Graduate College
of the Oklahoma State University
in partial fulfillment of the requirements
for the Degree of
MASTER OF SCIENCE
May, 1976

AN ENDOR INVESTIGATION OF THE V_K CENTER IN $KMgF_3$

Thesis Approved:

Larry E. Halliburton
Thesis Adviser

Dean of the Graduate College

ACKNOWLEDGEMENTS

To Dr. Halliburton, who patiently guided and advised me along the rocky road of ENDOR, I am greatly indebted. Without his help, I long ago would have quit the pursuit of this problem. Mr. Heinz Hall and Mr. Floyd Vulgamore's patience, with our incessant modifications, and machining expertise are greatly appreciated. I would also like to thank my parents for giving me the fortitude and encouragement necessary to complete six years of college.

Finally, I wish to thank my wife, Becky, for her sacrifice of our time together.

TABLE OF CONTENTS

LIST OF TABLES

LIST OF FIGURES

CHAPTER I

INTRODUCTION

Definition of Research Problem and Review of Literature

This thesis is primarily concerned with the development of an ENDOR spectrometer capable of measuring the hyperfine interaction of the intrinsic self-trapped hole (V_K center) in $KMgF_3$. Since the formation of a V_K center is one step in the commonly accepted primary production mechanism for F centers in halide materials, namely the Pooley-Hersh mechanism (1,2,3), its detailed structure is of great importance. An ENDOR investigation of the V_K center would determine the interactions of the unpaired electron with its surrounding ions. From these interactions an idea of the lattice distortion associated with the formation of a V_K center can be deduced.

Investigations have already been made for the intrinsic V_K centers in LiF (4), NaF (5), BaF_2 (6), and CaF_2 (6), and for the extrinsic V_{KA} center associated with Li in NaF (7). These investigations conclusively confirmed the V_K center model for those compounds and also showed that many of the ions surrounding the V_K center have negative contact terms. However, all of these ionic compounds have cubic type crystal structures. It would be of interest to determine if any important differences exist for V_K centers in lower symmetry crystal structures.

Recently, extensive work has been done on materials other than the alkalide halides to better understand the mechanisms of radiation induced damage. One of these materials is the perovskite $KMgF_3$ whose unit cell is given in Figure 1. T. P. P. Hall (8) has shown that in $KMgF_3$ V_K centers are formed between two of the six fluorine ions surrounding a center Mg^{2+} ion. These V_K centers were found to decay at 110 K and exhibit the bent bond configuration shown in Figure 1. This bent bond arises from the self-trapped hole being repelled from the double positively charged Mg^{2+} ion.

An interesting feature of the ESR spectrum is seen in Figure 2 for the 0^{o} lines with the magnetic field along the [110] direction. These lines exhibit a resolved structure which is attributed to interactions of the V_K center with the fluorine ions forming set A. Therefore, this result clearly shows that the ESR lines are broadened by interactions of the unpaired electron with nearest neighbor fluorine ions. The fact, that all V_K center ESR lines are inhomogeneously broadened, was discovered by Castner and Kanzig (9).

Of all the halides, only fluorine V_K centers have been investigated using ENDOR, because the ENDOR spectra from these V_K centers are both more easily detected and more easily interpreted. Fluorine has only one isotope having a spin of one-half. Thus, each inequivalent fluorine ion surrounding a V_K center will give rise to only two ENDOR lines. Furthermore, these ENDOR spectra are analyzed by diagonalization of the matrix representation of the spin Hamiltonian. Consequently, for smaller spin quantum numbers fewer eigenfunctions form the basis set used to make the matrix representation of the spin Hamiltonian. Therefore, the smaller the spin, the smaller the matrix representing the spin Hamiltonian. For

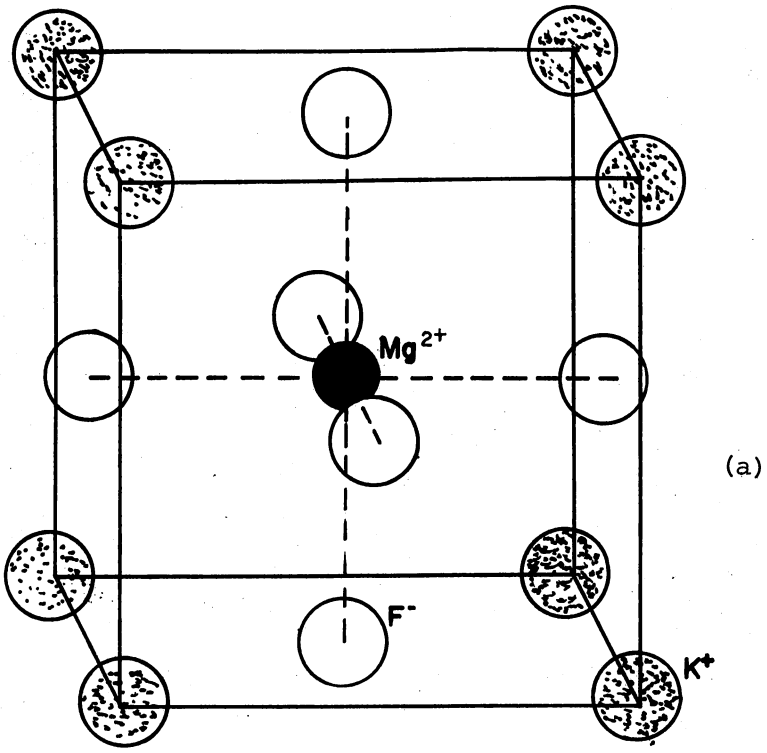

(a)

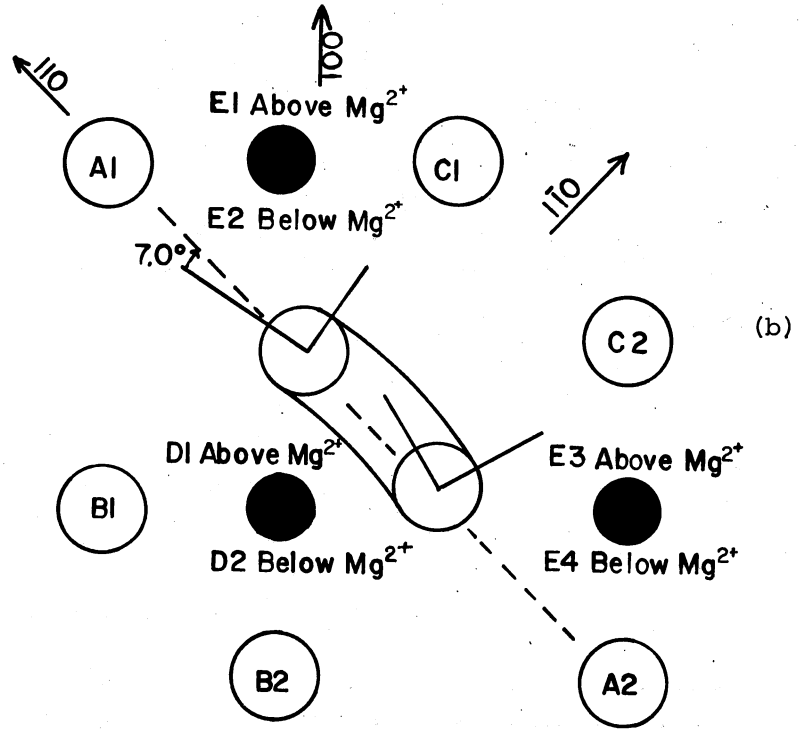

(b)

Figure 1. (a) Unit Cell for Cubic Perovskite $KMgF_3$.
(b) Geometry of V_K Center and Identification of Nearby Fluorine Ions

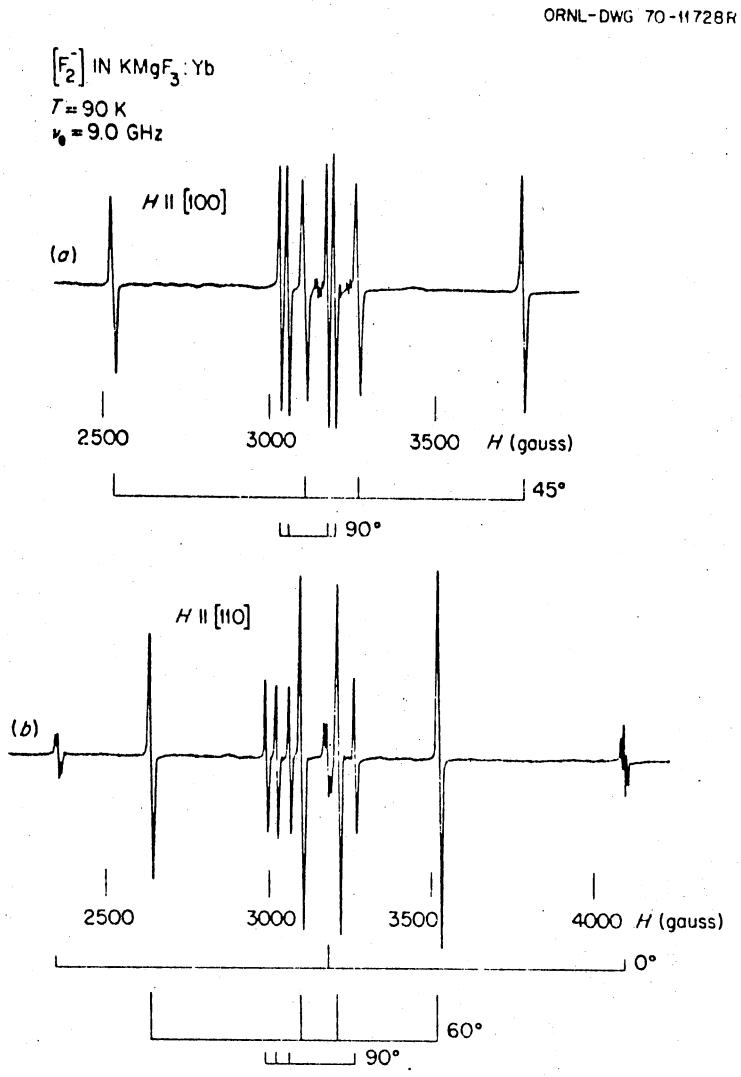

Figure 2. The [100] and [110] Spectra of the Intrinsic V_K Center in $KMgF_3$

instance, a 16 x 16 matrix is needed to represent a fluorine ion interacting with the unpaired electron of a fluorine V_K center, but a 128 x 128 matrix would be needed if chlorine were used. Since fluorine has a spin of one-half, it exhibits no quadrupole splitting of ENDOR lines to further complicate the ENDOR spectra. On the other hand, since no quadrupole terms can be determined for a spin one-half system, no information can be gained as to the electric field gradients at each fluorine site. Another consideration for studying fluorine ionic crystals is that the g value for a fluorine nucleus is much larger than the g value for the other halides. Thus, the nuclear Zeeman splitting in an applied magnetic field will result in a greater thermal spin population difference than if a nucleus of smaller g value were used. Since the size of an ENDOR signal is dependent upon the population differences between spin energy levels, fluorine ions would be expected to give the largest ENDOR signals.

Electron Nuclear Double Resonance (ENDOR)

To better understand the principles and prerequisites of ENDOR, a short description of the experiment is given in the next few paragraphs. More detailed descriptions can be obtained in the chapters on ENDOR in the selected references (10,11).

An ENDOR experiment is essentially the observation of a change in an ESR signal resulting from driving an NMR transition. Depending upon the relaxation times, two basic types of ENDOR experiments are possible. If the relaxation times are extremely long, the method of adiabatic fast passage can be used (12). For shorter relaxation times, the method of steady state ENDOR (13) is used. Since steady state ENDOR was used in

this investigation of the V_K center in $KMgF_3$, this type of ENDOR will be described in greater detail.

One of the greatest advantages of ENDOR is that it resolves inhomogeneously broadened ESR lines. An inhomogeneously broadened line is one which has a number of unresolved resonances, caused by small hyperfine interactions, contributing to the total line shape. This broadening of the ESR lines is not to be confused with broadening caused by fast relaxation processes. Therefore, an inhomogeneously broadened ESR line constitutes the first prerequisite for an ENDOR investigation.

Another condition for an ENDOR investigation is that an ESR signal must be able to be saturated. Saturation corresponds to the condition where the number of electrons in the $+\frac{1}{2}$ state approaches the number of electrons in the $-\frac{1}{2}$ state. To achieve saturation, the microwave power is increased until the ESR signal no longer increases. Since saturation can many times only be achieved at low temperatures with reasonable microwave powers, ENDOR is often done at liquid helium temperatures.

A further prerequisite for ENDOR is the ability to get a sufficient rf field on the sample. When the rf corresponds to the difference between energy levels obeying the selection rules $\Delta m_I = \pm 1$, $\Delta m_S = 0$, NMR transitions will occur. If these same levels have different electron spin populations, the rf can cause the electron spin populations to change for each level. Large rf fields are desired for ENDOR since ENDOR signals are proportional to the rf field until saturation of the NMR transitions is achieved. Above the saturation level, further increases in rf field will not increase the ENDOR signals.

Now the importance of saturation will become apparent. Remember, the saturated ESR electron spin states have a nearly equal amount of

electrons in the $+\frac{1}{2}$ state as in the $-\frac{1}{2}$ state. For the unsaturated transitions the number of electrons in the $+\frac{1}{2}$ state and the number of electrons in the $-\frac{1}{2}$ state is determined by a Boltzman distribution. Therefore, a greater electron spin population difference between energy levels exists for the unsaturated transitions than for the saturated transitions. If a $\Delta m_I = \pm 1, \Delta m_s = 0$ (NMR) transition occurs between a saturated energy level and an unsaturated energy level, the electron spin population differences between these energy levels will cause the formerly saturated ESR transition to become unsaturated and change the ESR signal's intensity. ENDOR is this change in the intensity of a saturated ESR transition caused by a NMR transition. It is strongly suggested that the reader refer to the selected references on ENDOR for a complete discussion of the population dynamics during an ENDOR experiment.

Since NMR transitions cause the observed changes in the ESR signal, the ENDOR spectra will obey $\Delta m_I = \pm 1$, $\Delta m_s = 0$ selection rules. If the hyperfine terms are smaller than the nuclear Zeeman interaction, as they are for V_K centers, the ENDOR lines will occur above and below the free spin frequency (the frequency a free nucleus would resonate in an applied magnetic field). However, if the hyperfine interaction is much larger than the nuclear Zeeman term, the ENDOR lines will be separated by the frequency corresponding to an energy $2g_n B_n H$.

From the discussion of the conditions necessary to observe ENDOR transitions, it was implied that the size of an ENDOR signal is dependent upon the induced electron spin population differences between energy levels of the formerly saturated ESR transitions. These population differences are dependent upon the spin lattice relaxation times of different energy levels and to the degree a NMR transition will change the

electron spin populations of the energy levels of the saturated ESR transition. Consequently, the size of an ENDOR signal is not a conclusive indicator of the degeneracy of a transition as is the case for ESR. In fact, sometimes ENDOR transitions are observed when neither of the energy levels corresponding to the NMR transition are the same energy levels which the saturated ESR transition connects. In such a case, the intensity of the ENDOR response is decreased and one could easily, wrongly, deduce that this line was less degenerate than other lines in the ENDOR spectra.

NMR on a crystal would have ions from different environments such as impurities as well as V_K centers resonating about the free spin frequency. Since ENDOR is only sensitive to ions strongly coupled to the V_K center, the ENDOR spectra will have many less lines than an NMR spectra. Consequently, even if NMR could be made sensitive enough to detect NMR transitions due to the surroundings ions of the V_K center, the NMR spectra would probably be too complex to interpret due to other defects in the crystal.

Summarizing, ENDOR represents a powerful technique which combines the sensitivity of ESR with the resolution of NMR. The necessary conditions for ENDOR to be observed illustrate the necessity for a versatile ENDOR spectrometer capable of varying temperature, rf and microwave power levels, and rf and static field modulations. Also, the size of an ENDOR signal does not necessarily indicate its degeneracy. Furthermore, ENDOR spectra vary depending upon the ratio of the hyperfine term compared to the nuclear Zeeman term.

CHAPTER II

APPARATUS AND EXPERIMENTAL PROCEDURE

Introduction to Instrumentation

A block diagram of the ENDOR spectrometer is given in Figure 3. Compared to most ENDOR spectrometers, this spectrometer is both a conceptually and instrumentally simple system. It utilizes an X-Band homodyne microwave bridge. To detect the ENDOR signal a double modulating scheme (14) is used; whereby the static magnetic field is amplitude modulated at 100 kHz and the rf is frequency modulated at 50 Hz. The high degree of coding produced by double modulation enables one to discriminate against appreciable noise. Furthermore, the frequency modulation of the rf results in very little baseline shift as compared to amplitude modulation. The static magnetic field modulation frequency can easily be modified to lower audio frequencies if desired for a particular ENDOR problem. The main problem with the ENDOR spectrometer is an inefficient utilization of rf power. Consequently, the rf power must be increased to a level where appreciable heating occurs. As with all ENDOR spectrometers, the ENDOR spectrometer does not have quite the sensitivity one desires.

Microwave Bridge

An X-band homodyne bridge, having both a bias and sample arm, was used in this ENDOR spectrometer. The sample arm contains a zero to 60

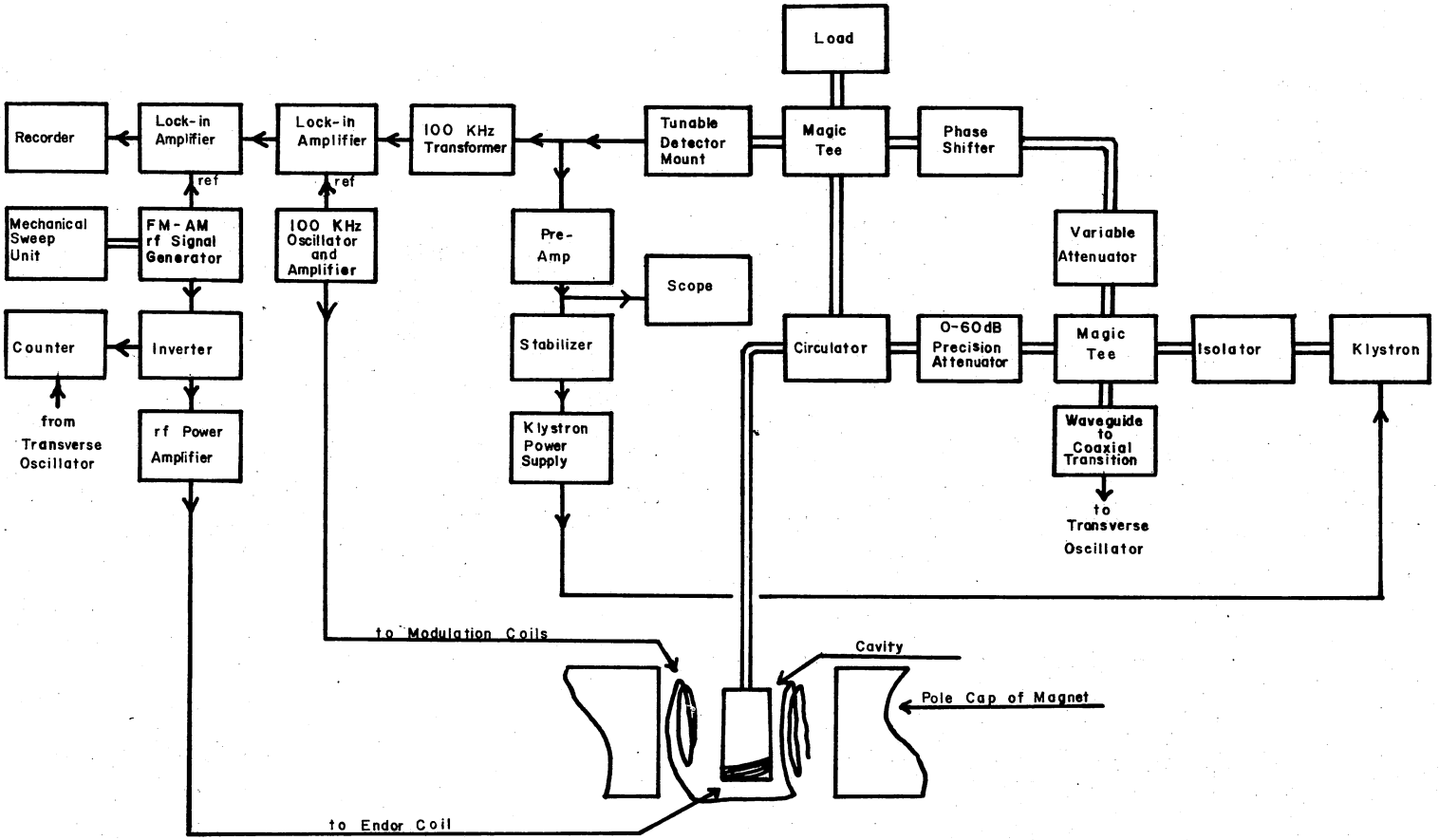

Figure 3. Block Diagram of ENDOR Spectrometer

dB precision attenuator to easily control the saturation level of the ESR transition.

A special low noise back diode from Microwave Associates was used as the detector diode for the microwave bridge. For this diode the inherent noise at 100 kHz was nearly equal to the inherent noise from a less expensive Schottky barrier diode. However, at lower frequencies, for instance 2 kHz, the back diode has much less inherent noise than the Schottky barrier diode. Since most ENDOR studies must be done at very low modulating frequencies in order to avoid passage effects, this type of diode is imperative. Passage effects are effects caused by the spin system not relaxing fast enough to follow the modulating field of the static magnetic field.

Detector System

As was stated previously, this ENDOR spectrometer employs a double modulation scheme to detect an ENDOR signal. The static magnetic field is amplitude modulated at 100 kHz while the rf is frequency modulated at 50 Hz. Therefore, the ESR transition is saturated and unsaturated at the frequency (100 kHz) of the static magnetic field modulation. Since an ENDOR response can only be observed when the ESR transition is saturated, an ENDOR signal results at a frequency of 100 kHz if only the one static magnetic modulation frequency is used. However, the rf is being frequency modulated at 50 Hz. Therefore, the resulting signal from the detector diode is a 100 kHz carrier along with sidebands, which contain the ENDOR information, at 99.95 kHz and 100.05 kHz.

This signal is then de-modulated and the ENDOR signal detected by use of two lock-in amplifiers in tandem. The detector diode is impedance

matched to a pre-amp by means of a tuned transformer (copied from the Varian Model 4560 modulation unit). Then the signal from the pre-amp is fed into a PAR 128 lock-in amplifier whose reference frequency is 100 kHz and whose time constant is on external. This lock-in amplifier detects the 100 kHz carrier, which is invarient, and also demodulates the side bands so that a 50 Hz signal results at the output of this lock-in amplifier. The signal from the PAR 128 lock-in amplifier is fed into a Keithley lock-in amplifier whose reference is at 50 Hz and time constant at 10 seconds. The 50 Hz ENDOR signal is detected in the second lock-in amplifier and recorded on a Leeds and Northrup recorder.

A static magnetic field modulation frequency of 100 kHz was used for its greater sensitivity and for its greater ease for operating the ENDOR spectrometer. If the first lock-in amplifier detects the static field modulation, one can easily oscillate between an ESR and ENDOR spectrometer by taking the output from either the first or second lock-in amplifier. When operating in the ENDOR mode, one can easily adjust the magnetic field to the field corresponding to the ESR transition by observing the meter on the first lock-in amplifier. Also, before the back diode was available, 100 kHz was used since we wished to operate at a frequency which minimized the inherent noise from the detector diode. The 50 Hz frequency modulation of the rf was used since the PAR 128 attenuated the sidebands associated with the higher rf modulating frequencies.

Static Magnetic Field Modulation

Because of the large ESR linewidth of the V_K center, an appreciable static modulating field must be attained. To produce this modulating

magnetic field, modulation was supplied by a set of Helmholtz oriented modulating coils which are tied onto the outside of the inner helium dewar. The power to these modulation coils was supplied by a 100 kHz oscillator and amplifier copy from the Varian Model V4560 modulating unit. The coils must be retied onto the dewar, following each immersion in liquid N_2, or they will vibrate and cause considerable microphonics. However, these coils were able to provide the necessary modulating static magnetic field into the cavity.

Cavity

The cavity used in this ENDOR investigation had to have the capabilities of being able to be irradiated at liquid nitrogen temperature since the V_K center decays at 110 K, be very reproducible ruling out placing the rf coils inside the cavity, and let about 12 Gauss of modulating field into the cavity since the linewidth of the ESR lines for the V_K center is near 12 Gauss. To achieve these goals a TE 102 rectangular cavity with three slots and an irradiation window was used (15,16) as shown in Figure 4. The three slots allowed both static magnetic field modulation and rf to enter the cavity. The rf enters the cavity when rf surface currents induced on the sides of the cavity flow through the slots to the inside of the cavity (17).

To supply the rf, a five turn coil of #30 magnet wire was wound around the outside of the lower end of the cavity. Since the coil is outside the cavity, it can not lower the Q of the cavity due to misorientation while the cavity was being mounted at liquid nitrogen temperature.

To enable the cavity to be mounted while the lower end was immersed

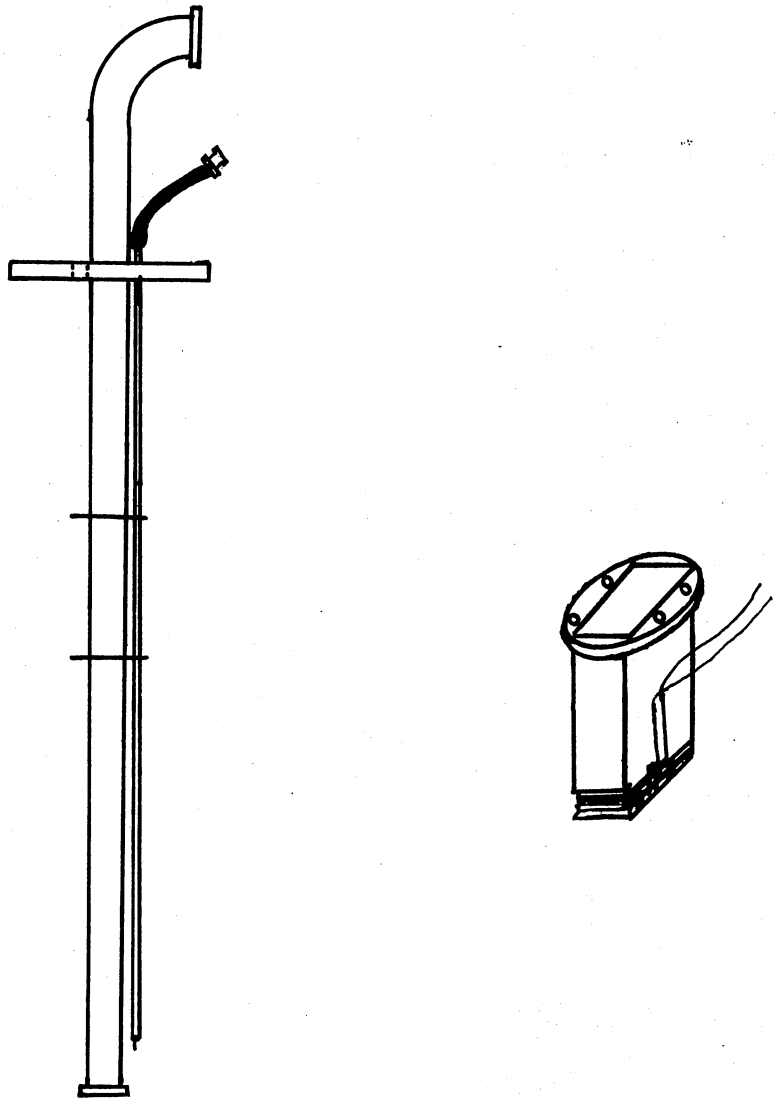

Figure 4. Cavity and Waveguide Connecting Cavity to Microwave Bridge

in liquid nitrogen, the holes at the upper flange of the cavity were threaded. Also, styrofoam filled the inside of the cavity to exclude liquid helium.

Waveguide

The waveguide connecting the cavity to the microwave bridge was designed to prevent a large heat leak into the inner helium dewar. To accomplish this goal, the waveguide was made of stainless steel (0.025 inches thick). Radiation baffles were placed eight and twelve inches from the top brass plate (see Figure 4) to shield the liquid helium from room temperature radiation. A thin walled stainless steel tube was used as the ground sheath for the coaxial cable transmission line leading to the five turn ENDOR coil around the cavity. In this way copper, which conducts heat well, usually used as the ground sheath was replaced by stainless steel which conducts heat poorly.

The capacitance, associated with the coaxial cable, was a problem since it and the inductance of the ENDOR coil formed a parallel resonance circuit. To give a more nearly constant rf power transfer to the ENDOR coil as a function of frequency, the center conductor and surrounding insulator of a low capacitance cable (RG 62/U, 13.5 μμF/Ft.) was strung through the thin-walled stainless steel tube. With this cable and five turn ENDOR coil a parallel resonance occurs at approximately 18 MHz.

Besides these design factors it was found necessary to ground the cable to the waveguide to prevent large baseline shifts in the ENDOR spectrum. Also, the waveguide was stuffed with styrofoam to exclude liquid helium.

R. F. System

A Hewlett Packard Model 202 H signal generator (56-216 MHz) was used to generate the 50 Hz frequency modulated rf signal. This unit is capable of both AM and FM at a number of internal frequencies and the frequency deviation of the F. M. can be varied from 0 - 250 kHz. This signal is fed into an univerter (HP Model 207H) and beat down to the frequency range (0.1 - 50 MHz). The resulting signal was fed into both a counter and a 50 watt linear power amplifier. The signal at the output of the power amplifier was fed through the previously described coaxial line to the ENDOR coil.

Sample Preparation

Two different crystal samples of $KMgF_3$ were used for the ENDOR experiments. Both crystals were grown by the Bridgeman-Stockbarger method in the crystal lab at Oklahoma State University. One of the sample's dimensions were 3 mm by 3 mm by 6 mm while the other sample's dimensions were 3 mm by 3 mm by 4 mm. Considerable effort was expended to get as large a sample as possible. Unfortunately, larger samples from crystals grown by the Bridgeman-Stockbarger method invariably contained more than one crystallite.

The impurity content of the two samples was quite different. The larger sample was quite impure in that the ESR signal due to Mn^{2+} was approximately the same intensity as the ESR signal due to the intrinsic V_K center. Consequently, when one wished to observe ENDOR responses from the ESR lines due to the V_K center in the region of the Mn^{2+} ESR signals, one could never be certain that the ENDOR spectra observed were due entirely to the V_K center and not to the Mn impurity. This fact

necessitated using the smaller sample which was doped with 60 ppm Li and had relatively little Mn impurity. Also the larger, highly impure sample had to be annealed after every irradiation or the number of V_K centers produced decreased for an unknown reason.

Crystal Mounting and Irradiation Procedure

To irradiate the samples, a procedure was used whereby the cavity with sample was irradiated at liquid nitrogen temperatures. Then the cavity was bolted to the waveguide while the lower end was immersed in liquid nitrogen since the intrinsic V_K center decays at 110 K.

The sample was mounted on a cleavage plane and adhered to the cavity (with silicon vacuum grease) either on one of the slots or next to the irradiation window. The size of the ESR signal, when the sample was mounted next to the irradiation window, was decreased by a factor of three when compared to the ESR signal from the same sample when mounted over one of the three slots. However, a more intense rf field was obtained for samples mounted next to the irradiation window when compared to samples mounted over one of the slots. In practice, the sample was usually mounted over the slot next to the irradiation window. After the crystal was mounted, styrofoam was stuffed into the rest of the cavity to exclude liquid helium.

The cavity was then placed in a cup filled with liquid nitrogen and the styrofoam cup was placed in a Co^{60} Gamma Cell (10^5 R/hr). Three hours of irradiation were needed to saturate the number of V_K centers which could be produced.

After irradiation, taking care that the cavity was always immersed in liquid nitrogen, the cavity and iris were bolted onto the waveguide.

Meanwhile, the inner dewar was cooled to near 77 K. The waveguide was quickly placed inside the inner dewar and a check was made to be certain that the resonance frequency of the cavity was within the klystron range. Then liquid helium was transferred into the inner dewar before the sample was able to warm up to 110 K.

Measurement of ENDOR Spectra

To find the [100] direction, ESR traces were taken of the low field line due to the molecular ion being orientated at a 45^{o} angle to the magnetic field. When the sample is slightly off angle from the [100] direction and the sample is mounted on a [100] plane, the line splits into 3 lines in a 1:2:1 ratio. Thus, the [100] direction could be found by adjusting the angle of the magnetic field till these three lines become degenerate. In a similar manner, the [110] direction was found by observing the low field line due to the molecular ion being orientated 60^{o} to the magnetic field. For this case, the ESR line splits into two equally intense lines. In Figure 2 the [100] and [110] ESR traces are shown.

After orientation of the sample was determined, the magnetic field was adjusted to the value corresponding to one of the peaks of the derivative of the ESR absorption curve. Each different orientation of a V_K center will give rise to a four line ESR spectra. However, each of these four lines contains exactly the same information about the hyperfine interaction of the surrounding ions of the V_K center with the unpaired electron. Consequently, it is only necessary to observe the ENDOR spectra on one of the ESR lines for each different orientation of the V_K center. Usually we chose a line that was not near the $g = 2$

region where the impurity Mn^{2+} ESR signals were appreciable. To determine the magnetic field, using a transfer oscillator, three beat frequencies of the microwave frequency were recorded, and the line width of the ESR line was recorded.

The microwave power was adjusted to the saturation level which maximized the ENDOR signal. The best ENDOR responses were found to be at microwave power levels of 25.5 dB for the smaller Li doped sample and 17 dB for the larger highly impure sample.

For the V_K centers in $KMgF_3$, a frequency deviation of 80 kHz was found to correspond to the approximate line width of the ENDOR lines. With this frequency deviation, little, if any, sensitivity was lost, and the ENDOR lines were still well resolved.

The mechanical sweep unit was operated at a 32/1 gear reduction ratio which corresponds to a sweep rate of 2.5 kHz per second. At this sweep rate the ENDOR lineshapes were not distorted. Slower sweep rates and longer time constants in the last lock-in amplifier could be used to improve the signal to noise ratio of the ENDOR signals, if the liquid helium did not evaporate so quickly.

The rf was swept decreasing and then swept increasing the frequency. Data taken in this manner can be reduced in such a way as to minimize systematic frequency shifts in the ENDOR line positions (refer to Chapter III, Section, Reduction of Data). Frequency markers were placed on the recorder chart by the operator while observing the radio frequency displayed on the counter.

CHAPTER III

ANALYSIS AND REDUCTION OF DATA

ENDOR line positions could only be taken along three highly degenerate angles of the magnetic field relative to the axis connecting the two fluorine nuclei of the V_K center. With the magnetic field in the [100] direction the V_K center axes form either 45° or 90° angles with the magnetic field in a ratio of 4:2, respectively. With the magnetic field in a [110] direction the V_K center axes form either 60°, 90°, or 0° angles with the magnetic field in a ratio of 4:1:1, respectively. Consequently, the ENDOR spectrum can most easily be obtained along the highly symmetrical directions where the static magnetic field is either 90°, 60° or 45° to the V_K center axis.

If one attempts to observe ENDOR spectra along a lower symmetry direction, the corresponding signal to noise ratio significantly decreases. For the most favorable directions for which ENDOR spectra have been taken, the typical signal to noise ratio was approximately 10:1. Therefore, since an arbitrary angle of the magnetic field to the V_K center has four times less V_K centers contributing to the ENDOR spectra, a signal to noise ratio of 2:1 or lower is expected. Thus, the sensitivity of our present ENDOR spectrometer is insufficient to attempt a complete angular study of the ENDOR line positions for the intrinsic V_K center in $KMgF_3$.

Reduction of Data

To analyze the ENDOR spectra, the magnetic field must be determined. The parameters of the ESR spin Hamiltonian of the intrinsic V_K center have already been determined (8) and can be described by a spin Hamiltonian of the form.

$$\hat{H} = \beta \vec{H} \cdot \tilde{g} \cdot \hat{\vec{S}} + \hat{\vec{I}}_i \cdot \tilde{A}_1 \cdot \hat{\vec{S}} + \hat{\vec{I}}_2 \cdot \tilde{A}_2 \cdot \hat{\vec{S}} - g_{nF}\, \beta_n\, \vec{H} \cdot (\hat{\vec{I}}_1 + \hat{\vec{I}}_2)$$

where

β = Bohr Magneton = 9.274096×10^{-21} erg/Gauss

$\hat{\vec{S}}$ = spin operator for unpaired electron

$\tilde{g}$ = g tensor for V_K center

$\tilde{A}_i$ = hyperfine tensor of either nucleous 1 or 2

$\hat{\vec{I}}_i$ = spin operator of nucleous 1 or 2

$g_{nF}\, \beta_n$ = gyromagnetic ratio of a flourine nuclei times Plank's constant divided by $2\pi = 2.654144 \times 10^{-20}$ erg/Gauss

The principle axes of the A tensor are defined in Figure 1. The tensors were found to have the values $g_x = 2.025$, $g_y = 2.018$, $g_z = 2.0024$, $A_x = 160$ MHz, $A_y = 160$ MHz and $A_z = 2479$ MHz.

Using these values and the measured microwave frequency, the magnetic field could be obtained by diagonalization of a 8 by 8 matrix representation of the spin Hamiltonian. A value of magnetic field was initially assumed at the input of a fitting program and adjusted until the measured microwave frequency and the calculated microwave frequency agreed. The actual magnetic field was not, however, the value calculated by the above fitting routine, but $\pm\frac{1}{2}$ the linewidth of ESR line being saturated depending on which peak of the derivative of the ESR

line one was observing.

The next step in analyzing ENDOR spectra is to calculate the difference between the measured frequency of an ENDOR line and the frequency at which a free fluorine nucleus would resonate due only to its magnetic moment. Since ENDOR is done by observing the change in intensity of an ESR line, obviously the magnetic field must be adjusted to the value of magnetic field corresponding to the ESR transition. However, the magnetic field at which an ESR transition occurs depends upon the angle the V_K center axis makes with the magnetic field. Therefore, in order to study the angular dependence of ENDOR lines, one must do ENDOR at varying magnetic fields. Since the hyperfine interaction is smaller than the nuclear Zeeman term, the ENDOR spectra will be centered about the free spin frequency which is determined by the magnetic field. Therefore, ENDOR spectrums, corresponding to different orientations of the V_K center, will be centered about varying frequencies. Thus, when analyzing line positions of an ENDOR spectrum, the difference between the observed ENDOR frequency and the free spin frequency must be determined if the angular dependence of the hyperfine interaction is to be studied.

The ENDOR line positions were experimentally determined by increasing and decreasing sweeps of the radio frequency. The average of each line position should then be taken to give the correct ENDOR line position. If the microwave frequency is different between the increasing and decreasing radio frequency ENDOR traces, the magnetic field will be different between the two ENDOR traces. Consequently, to compensate for the difference of magnetic field between the increasing rf trace and the decreasing rf trace, the difference between the ENDOR frequency and the free spin frequency should be the averaged quantity. By averaging the

ENDOR line positions with one of the methods described above, frequency shifts in ENDOR line positions (caused by the large time constants used in the last lock-in amplifier) are nullified.

In practice, none of the data was reduced completely with the prescribed method given above since no parameters could be determined and reduction of this data would merely waste computer time. However, the line positions experimentally measured are listed in Tables I, II and III along with the microwave frequency and line widths. This will provide a starting point for future calculations after a complete angular study can be made.

Analysis of Data

As shown in Figure 1, the surrounding fluorine ions can be grouped into five symmetry sets labeled A thru E. Each of the sets A, B and C has a plane of reflection symmetry, namely the mid-plane perpendicular to the [110] direction. Sets D and E have a plane of reflection both in the mid-plane perpendicular to the [110] direction and also a plane of reflection symmetry in the plane containing the V_K center. These five sets comprise the 12 nearest neighbor fluorine ions.

Even though no angular dependence of the ENDOR line positions could be made, by considering the symmetry of the ions surrounding the V_K center some conclusions can be drawn from the ENDOR spectra observed along the high symmetry directions.

For instance, Figure 5 shows that when the magnetic field is in a [001] direction and makes an angle of 90° to the V_K center axis, five pairs of lines are observed. This trace implies that five different ion sets are contributing to the ENDOR spectrum. For this orientation, each

TABLE I

ENDOR LINE POSITIONS TAKEN ON LOW FIELD 45° ESR LINE WITH MAGNETIC FIELD IN [100] DIRECTION

Trace Taken While Increasing rf		Trace Taken While Decreasing rf	
ENDOR Line Positions (MHz)	Microwave Frequency (GHz)	ENDOR Line Positions (MHz)	Microwave Frequency (GHz)
6.686	8.694	6.66	8.699
7.305	8.694	7.306	8.699
7.55	8.694	7.51	8.699
8.2	8.694	8.19	8.699
8.55	8.694	8.536	8.699
8.708	8.694	8.70	8.699
8.923	8.694	8.88	8.699
9.108	8.694	9.07	8.699
9.46	8.694	9.43	8.698
~ 9.926	8.694	~ 9.87	8.698
~10.1	8.694	~10.04	8.698
~10.47	8.694	~10.40	8.698
10.76	8.694	10.72	8.698
10.89	8.694	10.89	8.698
12.84	8.694	12.82	8.698
13.29	8.694	13.277	8.698

Line width of ESR line = 15 ±2 Gauss.

Magnetic Field = Calculated magnetic field + 7.5 Gauss.

TABLE II

ENDOR LINE POSITIONS TAKEN ON LOW FIELD 60° ESR LINE
WITH MAGNETIC FIELD IN [110] DIRECTION

Trace Taken While Increasing rf		Trace Taken While Decreasing rf	
ENDOR Line Positions (MHz)	Microwave Frequency (GHz)	ENDOR Line Positions (MHz)	Microwave Frequency (GHz)
6.869	8.742	6.82	8.741
8.756	8.737	8.725	8.740
8.82	8.737	8.78	8.740
9.40	8.740	9.34	8.740
10.054	8.741	9.996	8.739
10.24	8.741	10.21	8.739
10.7(?)	8.742	10.61(?)	8.739
11.51(?)	8.744	11.44(?)	8.739
-- (?)	--	11.61(?)	8.739
12.05	8.744	11.94	8.739
12.21	8.744	12.12	8.739
13.94	8.746	13.89	8.737
15.02	8.747	14.92	8.736
15.85	8.748	15.76	8.735
15.85	8.747	15.798	8.749

Line width of ESR line = 15 ±2 Gauss.

Magnetic Field = Calculated magnetic field + 7.5 Gauss.

TABLE III

ENDOR LINE POSITIONS TAKEN ON SECOND LOWEST FIELD 90° ESR LINE WITH MAGNETIC FIELD IN [001] DIRECTION

Trace Taken While Decreasing rf	
ENDOR Line Position (MHz)	Microwave Frequency (GHz)
9.759	8.807
10.066	8.807
10.49	8.807
10.87	8.807
11.2	8.806
12.705	8.806
13.238	8.806
14.046	8.806
~14.2	8.806
14.78	8.806

Line width of ESR line = 12 ±1 Gauss.

Magnetic Field = Calculated magnetic field + 6 Gauss.

Crystal mounted slightly off cleavage plane (< 2°).

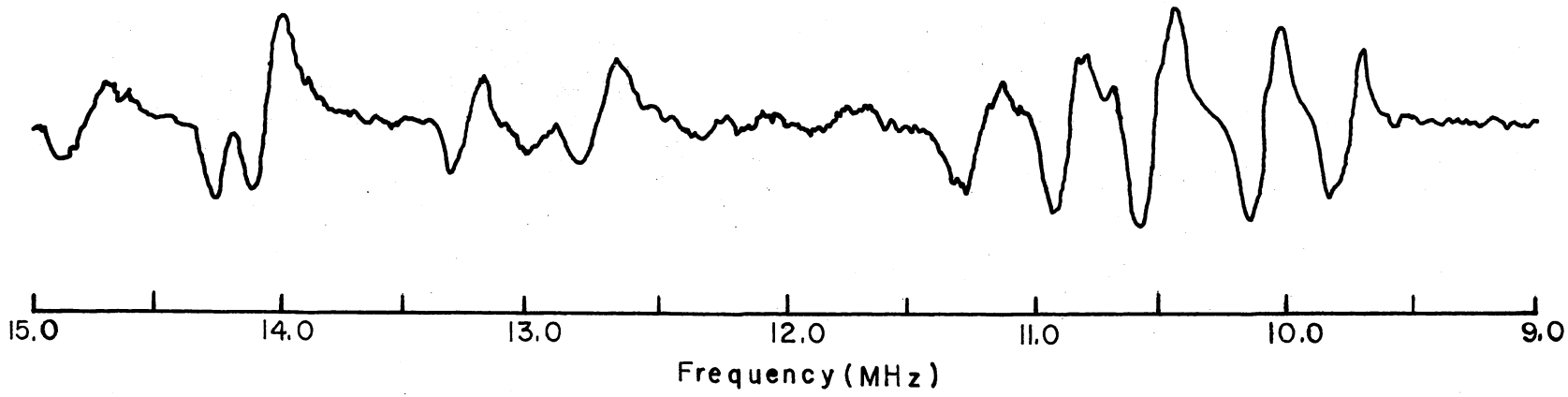

Figure 5. ENDOR Spectrum Observed While Saturating Second Lowest Field 90° ESR Transition With Magnetic Field in [001] Direction

member within a given set is equivalent and would give rise to an ENDOR spectrum consisting of five pairs of lines. Thus, one can conclude that the ENDOR lines observed are due only to the 12 nearest neighbor fluorine ions.

Furthermore, the set labeled D would be expected to have the largest hyperfine interaction in this orientation, since this set is closest to the V_K center and its principal axis is more nearly parallel to the magnetic field. Therefore, the outside lines of this spectrum are tentatively assigned to the set D fluorine ions. Even though the set A fluorine ions have a very strong hyperfine interaction with the V_K center, their strongest principal axis is known to be approximately along the [110] direction (8). Because the magnetic field is perpendicular to this direction, the hyperfine interaction due to set A would be weak in comparison to the D set. No further arguments about the relative magnitude and directions of the principal axes for the hyperfine tensors of the other sets can be made. Consequently, no further tentative line assignments can be made for this spectrum.

When the magnetic field is along the [100] direction but makes an angle of 45° with the axis of the V_K center, a 16 ENDOR line spectrum shown in Figure 6 is observed. In this orientation, the members contained in each set D and E are still equivalent. However, the members contained in each set A, B, and C become inequivalent. Therefore, as observed, eight inequivalent fluorine sites surround the V_K center and give rise to a 16 line ENDOR spectrum.

For the case where the magnetic field is 60° to the V_K center's axis, a 15 line ENDOR spectra is observed. For this orientation, the symmetry is entirely destroyed since, for all sets, the individual mem-

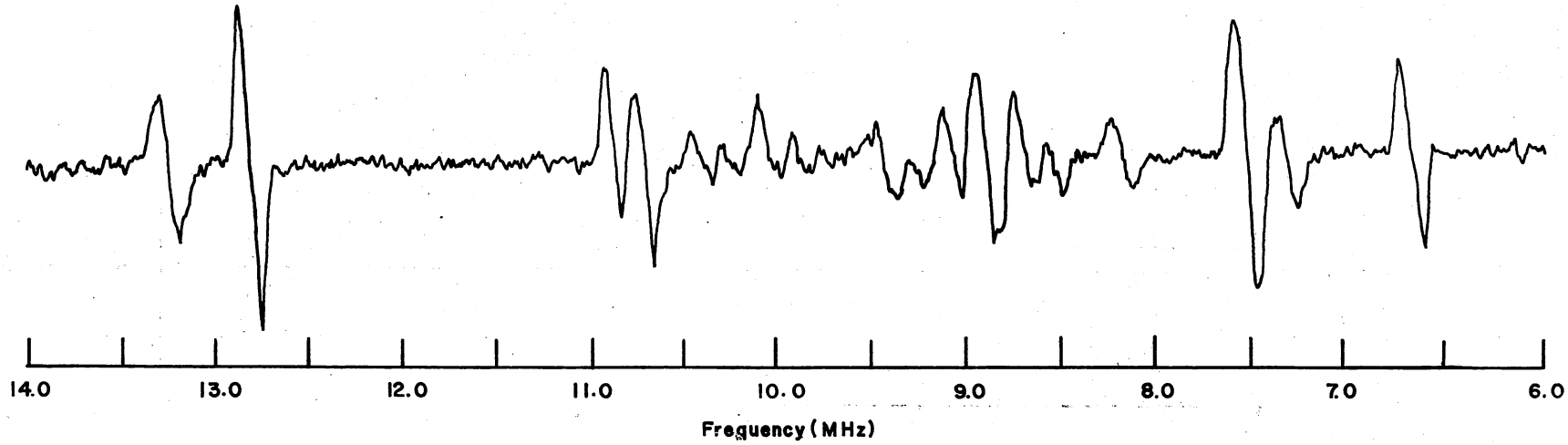

Figure 6. ENDOR Spectrum Observed While Saturating Low Field 45° ESR Transition With Magnetic Field in [100] Direction

bers contained in each set are inequivalent. The result is that 12 different fluorine ion sites surround the V_K center and should give rise to a 24 line spectrum. However, many of the lines are nearly degenerate and the resulting spectrum would not be expected to have 24 resolved ENDOR lines.

The [001] 90° spectrum has been identified as arising from five equivalent sets of ions. However, each pair of lines are observed not to be centered about the same frequency. Therefore, the "effective" free spin frequency is not the same for each set of ions. This effect can be explained by the effective magnetic field created by the unpaired electron of the V_K center. Since for inequivalent sites the effective magnetic field created by the unpaired electron is different, the pairs of lines would be expected to be centered about slightly different free spin frequencies. Furthermore, the electron interacting with the two fluorine ions which most strongly share the electron creates an effective magnetic field. This effective magnetic field is common to all the surrounding ions and depends upon the spin state of the V_K center. A detailed perturbation treatment of these effects is given by Gazzineli and Mieher (4).

Because of the fact that the ENDOR line positions depend upon the spin state of the V_K center, the spin Hamiltonian used to calculate the ENDOR line positions must be of the form $\hat{H} = \hat{H}_{ESR} + \hat{H}_{ENDOR}$. $\hat{H}_{ENDOR}$, alone, does not account for the effective field and therefore can not fit the data. $\hat{H}_{ESR}$ is the spin Hamiltonian previously given to calculate the magnetic field and $\hat{H}_{ENDOR} = \Sigma \hat{\vec{I}}_{ni} \cdot \tilde{A}_{ni} \cdot \hat{\vec{S}}$.

$\tilde{A}_{ni}$ = Hyperfine tensor of each fluorine ion surrounding the V_K center.

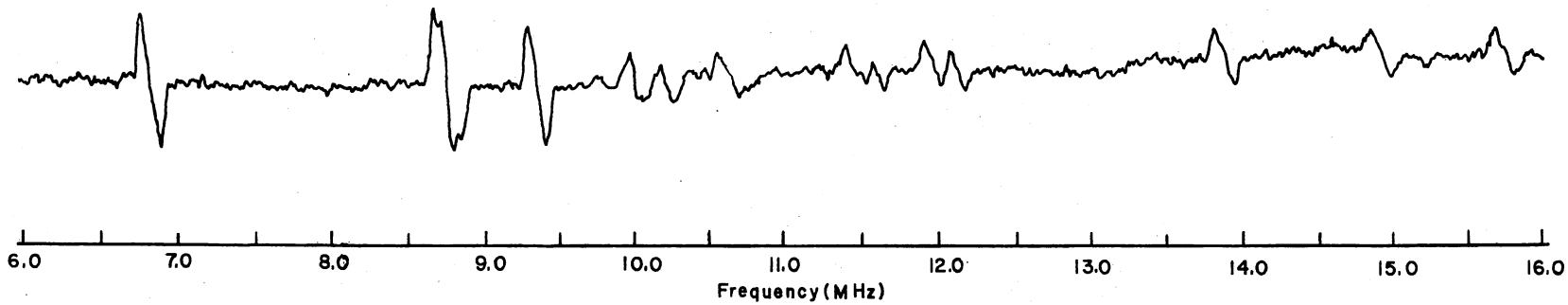

Figure 7. ENDOR Spectrum Observed While Saturating Low Field 60° ESR Transition With Magnetic Field in [110] Direction

$\hat{\vec{I}}_{ni}$ = Spin operator of each fluorine ion surrounding the V_K center.

To evaluate this spin Hamiltonian, each nuclei is treated as being independent of the spin state of the other ions surrounding the V_K center. For instance, the spin Hamiltonian for ion Al includes only the interaction of Al with the V_K center and not interactions of any other neighboring ions with V_K center. Before it was found that no complete angular data could be determined, a computer program was written to calculate the ENDOR line positions of sets A through D. Set E was not included since none of its principal axes directions could be deduced from symmetry considerations. Using the previously described spin Hamiltonian, ENDOR line positions were calculated using parameters given by Gazzeneli and Meiher (4) for the intrinsic V_K center in LiF. The predicted spectra exhibited the same gross behavior as our spectra. Thus no large differences are expected for the V_K center in $KMgF_3$ as compared to the V_K center in LiF.

CHAPTER IV

SUMMARY AND CONCLUSIONS

A homodyne ENDOR spectrometer using a double modulation detection scheme was developed, and ENDOR spectra for the intrinsic self trapped hole (V_K center) in $KMgF_3$ were observed. With this spectrometer, ENDOR spectra could only be observed along the high symmetry directions of the static magnetic field with respect to the axis of the V_K center. The ENDOR spectrum with the magnetic field along the [001] direction perpendicular to the V_K center axis could be explained as arising from interactions of the 12 nearest neighbor fluorine ions with the unpaired electron of the V_K center.

The sensitivity of the ENDOR spectrometer was insufficient to do a complete angular study. Consequently, no hyperfine parameters due to the ions surrounding the V_K center could be determined. A complete determination of the interaction of the surrounding ions of the V_K center with the unpaired electron awaits further improvement of the present ENDOR spectrometer. Appendix B discusses attempted modifications of the ENDOR spectrometer.

A SELECTED BIBLIOGRAPHY

(1) Pooley, D. Solid State Communications, 3, 241 (1965).

(2) Sonder, E., and W. A. Sibley, "Defect Creation by Radiation in Polar Crystals." Point Defects in Solids, Volume I, General and Ionic Crystals. J. H. Crawford, Jr., and L. M. Slifkin, eds., New York: Plenum Press, 1973, pp. 201-283.

(3) Crawford, J. H., Adv. Phys. 17, 93 (1968).

(4) Gazzinelli, R. and R. L. Mieher, Phys. Rev. 175, 395 (1968).

(5) Daly, D. F. and R. L. Mieher, Phys. Rev. 175, 412 (1968).

(6) Marzke, R. F. and R. L. Mieher, Phys. Rev. 182, 453 (1969).

(7) Bass, I. L. and R. L. Mieher, Phys. Rev. 175, 421 (1968).

(8) Hall, T. P. P., Brit. J. Appl. Phys. 17, 1011 (1966).

(9) Castner, T. G., and W. Känzig, J. Phys. Chem. Solids 3, 178 (1957).

(10) Wertz, J. E. and J. R. Bolton. Electron Spin Resonance: Elementary Theory and Practical Applications. New York: McGraw-Hill Book Company, 1972, pp. 353-376.

(11) Abragam, A., and B. Bleany. Electron Paramagnetic Resonance of Transition Ions. Oxford: Clarendon Press, 1970, pp. 217-274.

(12) Feher, G., Phys. Rev. 114, 1219 (1959).

(13) Seidel, H., Z. Physik, 165, 218 (1961).

(14) Ranon, V. and J. S. Hyde, Phys. Rev. 41, 259 (1966).

(15) Holton, W. C., and M. Blum, Phys. Rev. 125, 89 (1962).

(16) Unruh, W. P. and J. W. Culvahouse, Phys. Rev. 154, 861 (1967).

(17) Nelson, L. "Electron Nuclear Double Resonance in Electron-Irradiated MgF_2." Microfilm copy (Unpub. Ph.D. dissertation, Library, Ohio University, 1973), pp. 41-43.

APPENDIX A

ANALYSIS OF ENDOR SPIN HAMILTONIAN

To analyze this spin Hamiltonian all the tensors must be transformed to the coordinate system where z is defined to be the direction of the magnetic field. To understand how this transformation is done, consider the total spin Hamiltonian needed to analyze the ENDOR data.

$$\hat{H} = \beta \vec{H} \circ \tilde{g} \cdot \hat{\vec{S}} + \hat{\vec{I}}_1 \cdot \tilde{A}_1 \cdot \hat{\vec{S}} + \hat{\vec{I}}_2 \circ \tilde{A}_2 \cdot \hat{\vec{S}} + \hat{\vec{I}}_{ni} \circ \tilde{A}_{ni} \cdot \hat{\vec{S}}$$
$$- g_{nF} \beta_n \vec{H} \cdot (\hat{\vec{I}}_1 + \hat{\vec{I}}_2 + \hat{\vec{I}}_{ni}) \qquad (1)$$

Define the rotational matrices as follows.

$\begin{pmatrix} x \\ y \\ z \end{pmatrix}$ crystal coordinate system $= \tilde{R}$ $\begin{pmatrix} x \\ y \\ z \end{pmatrix}$ magnetic field coordinate system (direction of magnetic field is z)

$\begin{pmatrix} x \\ y \\ z \end{pmatrix}$ principle axes of A_1 tensor $= \tilde{T}_1$ $\begin{pmatrix} x \\ y \\ z \end{pmatrix}$ crystal coordinate system $= \tilde{T}_1 \tilde{R}$ $\begin{pmatrix} x \\ y \\ z \end{pmatrix}$ magnetic field coordinate system

$\begin{pmatrix} x \\ y \\ z \end{pmatrix}$ principle axes of A_2 tensor $= \tilde{T}_2$ $\begin{pmatrix} x \\ y \\ z \end{pmatrix}$ crystal coordinate system $= \tilde{T}_2 \tilde{R}$ $\begin{pmatrix} x \\ y \\ z \end{pmatrix}$ magnetic field coordinate system

$\begin{pmatrix} x \\ y \\ z \end{pmatrix}_{\text{principle axes of } A_{ni} \text{ tensor}} = \tilde{T}_{ni} \begin{pmatrix} x \\ y \\ z \end{pmatrix}_{\text{crystal coordinate system}} = \tilde{T}_{ni}\, \tilde{R} \begin{pmatrix} x \\ y \\ z \end{pmatrix}_{\text{magnetic field coordinate system}}$

Using these rotation matrices, the spin Hamiltonian (Eqn. 1) becomes in the coordinate system where z is defined to be the direction of the magnetic field

$$\hat{H} = \beta \vec{H} \cdot \{\tilde{R}^{-1} \tilde{g} \tilde{R}\} \cdot \hat{\vec{S}} + \hat{\vec{I}}_1 \cdot \{(\tilde{T}_1 \tilde{R})^{-1} \tilde{A}_1 (\tilde{T}_1 \tilde{R})\} \cdot \hat{\vec{S}}$$

$$+ \hat{\vec{I}}_2 \cdot \{(\tilde{T}_2 \tilde{R})^{-1} \tilde{A}_2 (\tilde{T}_2 \tilde{R})\} \cdot \hat{\vec{S}} + \hat{\vec{I}}_{ni} \cdot \{(\tilde{T}_{ni} \tilde{R})^{-1} \tilde{A}_{ni} (\tilde{T}_{ni} \tilde{R})\} \cdot \hat{\vec{S}} \qquad (2)$$

$$- g_{nF} \beta_n \vec{H} \cdot (\hat{\vec{I}}_1 + \hat{\vec{I}}_2 + \hat{\vec{I}}_{ni})$$

Now, a spin operator (J_x, J_y, J_z) is transformed into the raising and lowering operators by the transformation

$$\begin{pmatrix} J_x \\ J_y \\ J_z \end{pmatrix} = \tilde{O} \begin{pmatrix} J_+ \\ J_- \\ J_z \end{pmatrix} \qquad \tilde{O} = \begin{pmatrix} \frac{1}{2} & \frac{1}{2} & 0 \\ \frac{1}{2i} & \frac{-1}{2i} & 0 \\ 0 & 0 & 1 \end{pmatrix}$$

This transformation is substituted into Eqn. 2 to finally give the spin Hamiltonian in the magnetic field coordinate system and in terms of the spin operators (J_+, J_-, J_z).

$$\hat{H} = \beta \vec{H} \cdot \{(\tilde{R})^{-1} \tilde{g}(\tilde{R}) \tilde{O}\} \cdot \hat{\vec{S}} + \hat{\vec{I}}_1 \cdot \{\tilde{O}^T (\tilde{T}_1 \tilde{R})^{-1} \tilde{A}_1 (\tilde{T}, \tilde{R} \tilde{O})\} \cdot \hat{\vec{S}}$$

$$+ \hat{\vec{I}}_2 \cdot \{\tilde{O}^T (\tilde{T}_2 \tilde{R})^{-1} \tilde{A}_2 (\tilde{T}_2 \tilde{R} \tilde{O})\} \cdot \hat{\vec{S}} + \hat{\vec{I}}_{ni} \cdot \{\tilde{O}^T (\tilde{T}_{ni} \tilde{R})^{-1} \tilde{A}_{ni} (\tilde{T}_{ni} \tilde{R} \tilde{O}) \cdot \hat{\vec{S}}$$

$$- g_n \beta_n \vec{H} \cdot \{\hat{\vec{I}}_1 + \hat{\vec{I}}_2 + \hat{\vec{I}}_{ni}\} \qquad (3)$$

Using the above spin Hamiltonian a 16 by 16 matrix representation is

diagonalized by computer to obtain the eigenvalues. The appropriate eigenvalues are subtracted, taking into account the selection rule $\Delta m_I = \pm 1$ and the ESR line being saturated, to find the ENDOR frequencies.

APPENDIX B

MODIFICATION OF PRESENT ENDOR SPECTROMETER

A number of attempts were made to improve the sensitivity of this ENDOR spectrometer. To aid others who may also try these modifications, they are discussed in the following paragraphs.

Many variations, all of which proved unsatisfactory, for both rf and static field modulation were tried. The first of these was to only modulate the rf and not modulate the static field at all. No matter if the rf was frequency modulated or amplitude modulated, no ENDOR signal could be seen from the test sample of irradiated MgO. When the rf was amplitude modulated instead of frequency modulated, while the static magnetic field was being modulated, the sensitivity was found to decrease substantially. Finally, the rf was both amplitude modulated and frequency modulated with the static magnetic field also being modulated. For this scheme no improvement was found over double modulation.

A teflon filled cylindrical cavity was made for the usual increase in Q of a cylindrical cavity as compared to a rectangular cavity. To admit static field modulation and also rf into the cavity, slots were cut through the walls in a manner which did not interrupt microwave surface current flow in the cavity. An ENDOR coil was wound around the belly of the cavity but little, if any, rf penetrated into the cavity. Furthermore, the Q of the cavity was significantly decreased by the slots cut through the cavity walls.

To increase the rf field incident on the sample, a 50 watt power amplifier instead of a 12 watt power amplifier was used to supply power to the ENDOR coils. While this power amplifier did increase the field inside the cavity and consequently improve the ENDOR signals, it also caused the liquid helium to boil away much more rapidly. Also, as a test, when a coil was wound directly around a sample, it was found possible to saturate the ENDOR transitions with sufficient rf power.

If the sample size is kept constant, a factor of 22 increase can be gained by increasing the microwave frequency from X-band to K-band. With this fact in mind, a cylindrical K-band cavity was designed where the coil was wound over the sample. Since a K-band cavity is much smaller than an X-band cavity, it does not need to be filled with teflon to reduce the cavity dimensions. The major problem encountered with the cavity was that an approximate maximum of 1 Gauss of 100 KHz static field modulation would penetrate into the cavity. This result implies that much lower static field modulation frequencies must be used. Since a low noise back diode is not manufactured for K-band, the inherent 1/f noise of a contact diode increases to a level where the sensitivity gained switching to K-band is lost by the necessary decrease in static magnetic field modulating frequency. Perhaps a wire wound cylindrical cavity or an extremely thin-walled cavity could be made to better admit 100 KHz static magnetic field modulation. One further problem with operating at K-band frequencies is that doped $KMgF_3$:Li samples, which were not lossy at X-band frequencies, became lossy at K-band frequencies.

VITA

Eugene Philip Little

Candidate for the Degree of

Master of Science

Thesis: AN ENDOR INVESTIGATION OF THE V_K CENTER IN $KMgF_3$

Major Field: Physics

Bibliographical:

Personal Data: Born in Watertown, South Dakota, June 28, 1952, the son of Philip and Phyllis Little.

Education: Graduated from Watertown Senior High School, Watertown, South Dakota, in June, 1970; received the Bachelor of Science with a major in physics from South Dakota State University in May, 1974; completed requirements for the Master of Science degree at Oklahoma State University in May, 1976.